J. Phys. Chem. A **2004,** *108,* 7527−7534

Low-Temperature Reactions of OH Radicals with Propene and Isoprene in Pulsed Laval Nozzle Expansions

Tim Spangenberg, Sven Köhler, Björn Hansmann, Uwe Wachsmuth,[†] and Bernd Abel*

Institut für Physikalische Chemie, Universität Göttingen, Tammannstasse 6, D-37077 Göttingen, Germany

Mark A. Smith

Department of Chemistry, University of Arizona, Tucson, Arizona 85721

Received: November 5, 2003; In Final Form: June 15, 2004

The kinetics of the reactions of OH radicals with propene and isoprene in N_2 have been studied in the temperature range of 58−300 K in a Laval nozzle expansion. Laser-induced fluorescence of the OH radical that is formed in the photolysis of H_2O_2 at 193 nm has been detected. The determined rate constants (2×10^{-11} to 2×10^{-10} cm^3 $molecule^{-1}$ s^{-1}) for the OH radicals reacting with excess propene and isoprene (2-methyl-1,3-butadiene) have been found to increase when the temperature is decreased. The room temperature rate constants are in agreement with the literature data. Below 120 K, a saturation of the rate constant for the case of propene and a turnover to a formally positive temperature dependence for isoprene have been observed. The observed negative temperature dependence and the course of the temperature dependence at very low temperatures for both reactions are discussed within the framework of the loose transition-state theory and a simple two-transition-state model.

I. Introduction

Low-temperature kinetic studies are both fundamentally interesting and important for understanding atmospheric chemistry,[1,2] reactions in the atmospheres of other planets,[3] and the chemistry in interstellar clouds.[4] To model the processes in these low-temperature environments, researchers often have to extrapolate the high-temperature kinetic data from elementary reactions to lower temperatures over a large range.[2] For many reactions between neutral species, the rate constants exhibit non-Arrhenius behaviors at low temperatures; for example, they have rate constants that increase as the temperature is lowered. The recognition that the potential energy hypersurfaces for such reactions do not possess significant potential barriers along their minimum energy paths has stimulated the development of theoretical capture models on the basis of the loose transition-state theory. An important motivation for measuring the rate data at very low temperatures beyond their direct application and use in large-scale models for describing atmospheric and interstellar chemistry is to test such models.[5,6] In fact, at very low temperatures, the rate constants of chemical reactions are very sensitive to the subtle features of the underlying potential energy surface in the most chemically relevant regions.

The investigation of rate constants at temperatures lower than room temperature was limited for quite some time to temperatures above 200 K. In these experiments, the low temperatures were achieved by the cryogenic cooling of the pulsed photolysis or discharge−flow systems. In the studies of gas-phase processes, cryogenic cooling has an obvious limitation: the condensation of the reacting species in the gas mixture. In addition, experiments below 200 K were limited in the past due to the low vapor pressure of many reagents. An experimental approach for low-temperature studies enables us to circumvent these limitations by using Laval nozzle expansion setups, which may be regarded as flow reactors without walls.[7−9] The development and application of this technique have been pioneered by Rowe and co-workers[7,10−13] and, later, by Smith and Sims.[2] They invented the abbreviation CRESU (Cinétique de Réaction en Ecoulement Supersonique Uniforme) for the Laval nozzle expansion technique. A Laval nozzle, first used in wind tunnels and aerodynamics investigations, produces a uniform expansion with a constant Mach number. It has a converging−diverging channel that has to be designed and precisely manufactured for each temperature and particle density, producing a uniform gas flow with no or negligible temperature or density gradients and a well-defined thermal low-temperature environment in the flow after the nozzle exit.[8] Currently, the Laval nozzle expansion-type apparatus is the only instrument capable of measuring the rate constants of molecules at temperatures as low as 10 K without the condensation of low-vapor pressure reagents occurring. Such systems have been used for studying ion−molecule reactions[10−13] and neutral−neutral reactions by the use of pulsed-laser photolysis in combination with laser-induced fluorescence[4,14,15] or chemiluminescence.[16,17] The systems employed by the groups of Rowe and Smith were continuous flow systems that required large pumping capacities. Recently, Smith's group developed a pulsed Laval expansion apparatus that requires a much smaller pumping system.[8] Using a cold cathode discharge source for the radicals and a LIF detection, they were able to demonstrate the power of the setup and to study several radical−molecule reactions.[18,19] Typical densities are 10^{15}−10^{17} cm^{-3}, and temperatures range from 10 to 300 K. Within the past two years, Leone et al. developed a pulsed Laval nozzle machine and published several applications.[3,9,20−23]

---

* Corresponding author. E-mail: babel@gwdg.de.

[†] Present address: Laser-Laboratorium Göttingen e.V., Hans-Adolf-Krebs-Weg 1, D-37077 Göttingen, Germany.

10.1021/jp031228m CCC: $27.50

SCHEME 1: Isomers of the Adducts Formed in the Primary Addition of OH to Propene (A) and Isoprene (B)

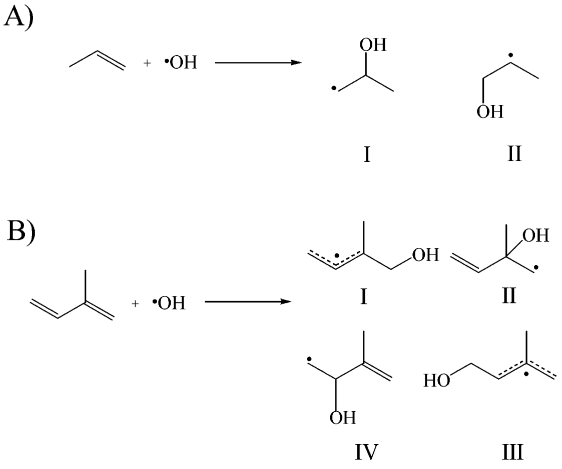

In the present article, we describe the newly developed pulsed Laval nozzle expansion setup that has been combined with laser-flash photolysis and laser-induced fluorescence for the detection of radicals. It has been used here for studying the reactions of OH radicals with two unsaturated hydrocarbons. The reactions of OH radicals with propene and isoprene in nitrogen buffer gas have been chosen for a number of reasons (see Scheme 1). The OH radical is one of the most important species in the atmosphere due to its ability to oxidize a large number of organic species. It is easy to detect via laser-induced fluorescence and constitutes a nearly ideal reagent because OH radicals can be generated conveniently by photolysis in the UV spectral range, for example, at 193 or 248 nm. Despite the low total pressure in the experiments, the temperature is low enough and the product radicals are large enough for these association reactions to be at, or very close to, their high-pressure limits. Since we only measured the decay and not the possible intermediates or products in the experiments, we cannot judge a priori what reactions contribute to the decay of the OH. In principle, a competing reaction channel could be the H atom abstraction, but it is, however, unlikely and should not play a significant role in the systems and experimental conditions (temperatures) investigated here.[24,25]

The reaction of OH radicals with propene (Scheme 1A) was investigated by Tully and Goldsmith[26] at high temperatures and recently by Leone and co-workers[3,23] at temperatures between 96 and 296 K. Therefore, we regarded it to be a good test system for our apparatus. Our initial goal was to extend the range of measured rate constants to lower temperatures and to investigate whether the trend of the negative temperature dependence continues at lower temperatures. In addition, we found the reaction interesting because it is one of the simplest recombination reactions in which different isomers of the intermediate adduct are formed (see Scheme 1A), which may display different kinetics at different temperatures, which may show up in the decay of the OH radicals.

Isoprene is the major biogenic non-methane hydrocarbon in the atmosphere. It is emitted by a wide variety of plants during daylight.[27] It plays an important role in ozone formation in the local and regional atmosphere due to its high chemical reactivity, and it is important in the generation of peroxy radicals. Since isoprene is emitted only during daylight hours, the reaction with OH is expected to be the dominant tropospheric removal pathway. The first step in the oxidation of isoprene occurs predominantly via the addition of the hydroxyl radical, OH, to one of the four sites, resulting in the four possible isoprene−OH adducts shown in Scheme 1B. Although the oxidation of isoprene involves many subsequent reaction steps, the initial isomeric branching of the isoprene−OH adducts may strongly influence the final product distribution (methyl vinyl ketone, methacrolein, formaldehyde, or 3-methylfuran).[28,29] With respect to the previous case (propene), we found it very interesting that in the OH−isoprene reaction four intermediate adduct isomers[30] can be formed that may, in principle, display a characteristic temperature dependence.

TABLE 1: Different Nozzles Employed in the Present Study

nozzle	temperature (K)	flow density ($\times 10^{17}$ cm^{-3})	Mach number
M21	114	1.0	2.1
M27	101	0.5	2.7
M35	84	1.0	3.5
M40	71	0.9	4.0
M50	58	0.6	5.0

Several laboratory experiments have reported temperature-dependent rate constants from the reaction of isoprene with OH and have identified the major reaction products.[31−33] Recent laboratory measurements of the rate constant of reaction B in Scheme 1 showed a negative temperature dependence between 250 and 400 K.[34−36] The question is, however, whether the rate constants continue to increase at much lower temperatures.

The present article is the first of a series that systematically explores the features and rate constants of OH reactions with a number of unsaturated hydrocarbons of different complexity (including aromatic systems) at very low temperatures.

II. Experimental Section

A. Experimental Setup. A CRESU apparatus creates a supersonic gas flow, employing a specially designed Laval nozzle. The Laval nozzle is a convergent−divergent shaped nozzle that accelerates a carrier gas to a certain Mach number. A new nozzle is required for each temperature/pressure pair and for a particular carrier gas. Five different Laval nozzles have been designed according to the method of Moger and Ramsay[8,37] taking into account the boundary layer and manufactured in our workshop to access a set of temperatures between 58 and 300 K. The different Laval nozzles (and their parameters) employed in the present study are summarized in Table 1. The nozzles are mounted on a stainless steel block that can be moved across a range of 15 cm along the axis of the gas flow. The Laval nozzle is directly mounted to a stagnation reservoir which has a volume of less than 1 cm^3 to ensure constant pressure conditions during each pulse. The stagnation reservoir is fed by two pulsed valves perpendicular to the beam axis. One of them has a 3 mm orifice to ensure sufficient carrier gas flow (a home-built fuel injection nozzle, BOSCH), whereas the other one, a General Valve Series 9 valve (400 μm), provides the reagent gas that is typically premixed in a stainless steel gas cylinder. Gas pulses have a duration of 7 ms to ensure constant and stable flow conditions. Hydrogen peroxide is mixed into the carrier gas flow by bubbling nitrogen through a fritted wash bottle. The concentration of the hydrogen peroxide solution was typically higher than 90%. The gas supply is controlled and measured by two mass flow controllers (Tylan) and pressure gauges in front of the valves. The mass flow controllers are calibrated by passing the gas into a known volume and recording the pressure increase. From the settings of the mass flow controllers and the known gas density in the flow, we were able to calculate the concentration of the excess reagent. OH radicals were produced via the photolysis of H_2O_2 at 193 nm. Absorption cross sections and quantum yields for H_2O_2 pyrolysis at 193

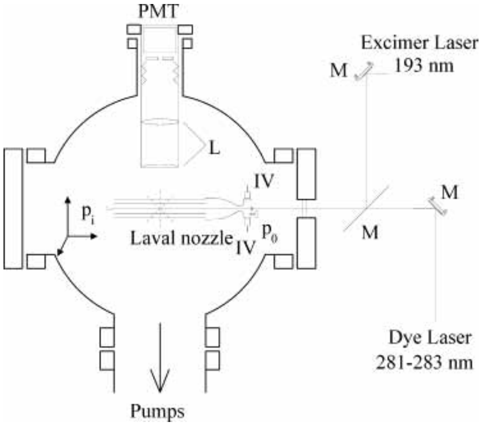

Figure 1. Laval nozzle expansion apparatus used for the present experiments. (PMT) photomultiplier tube, (L) lenses, (M) mirrors, (IV) injection valves, and (p_0 and p_i) stagnation and impact pressure gauges, respectively. Quartz windows in the chamber exits and in the backside of the stagnation reservoir of the Laval nozzle were used to direct the laser beams through the vacuum chamber, overlapping completely with the cold core of the gas flow. In this geometry, the delay between the two laser pulses defined the delay time of the experiment.

nm for the determination of OH concentrations were taken from the literature.[38-40] A comparison of experiments that were performed at a photolysis wavelength of 248 and 193 nm showed the same results.[41] In addition, the good agreement of our present results with those of Leone et al.,[3] employing a 248 nm wavelength for the generation of OH radicals from H_2O_2, demonstrates the equivalence of both sources in the experiments described here.

The pressure in the stagnation region (p_0), the impact pressure (p_i) downstream of the flow, and the background pressure (p_{bg}) in the reaction chamber were recorded. The background pressure is adjusted through an inlet valve of the vacuum chamber to control the desired uniform flow conditions. The pumping capacity of the main roots pump was about 400 $m^3\ h^{-1}$, which was found to be sufficient for the present experiments.

The optical system consists of an excimer laser operating at 193 nm (Lambda Physik EMG 101 MSC) and a Nd:YAG (Spectra-Physics Quanta Ray GCR-150, second harmonic) pumping a frequency-doubled dye laser (Lambda Physik Scanmate 2E) with a Rhodamine 6G (ethanol) solution. Quartz windows were mounted at the end of the chamber and at the backside of the stagnation reservoir to overlap the two laser beams collinearly within the center of the cold gas flow. In this geometry, the delay between the two laser pulses defined the delay time of the experiment. The laser-induced fluorescence from the $Q_1(1)$ line of the (1,0) band of the $A^2\Sigma \leftarrow X^2\Pi$ electronic transition of the hydroxyl radical was spatially imaged from a narrow region of the low-temperature gas beam. After passing through an f:1 optics, a filter, and an aperture, the fluorescence light was detected with a photomultiplier (EG&G PARC 4121B). The signal was fed into a Boxcar integrator and was averaged 10−20 times in a desktop computer in order to obtain an acceptable signal-to-noise ratio. The experiment was carried out at 10 Hz and controlled by two Stanford Research Systems delay generators (DG535). The time resolution was set to 1 μs, and a negative time delay of 10 μs was recorded prior to each experiment. The apparatus used in the present experiments is schematically shown in Figure 1. Hydrogen peroxide (70%) was obtained from Solvay Interox and concentrated up to 90% by bubbling nitrogen through it overnight. Propene (99.5%) and isoprene (≥98%) were purchased from Messer Griesheim and Fluka and were used without further purification.

B. Characterization of the Flow Conditions. From the dynamic pressure measurements, the conditions in the gas flow could be characterized. This is an essential step in the experiments because it ensures stable and well-defined uniform conditions. The stagnation pressure p_0, the impact pressure p_i, and the background pressure p_{bg} were measured to control and optimize the flow conditions. The Rayleigh formula has been used to calculate the Mach number of the supersonic flow according to

$$\frac{p_i}{p_0} = \left[\frac{(\gamma + 1)M^2}{(\gamma - 1)M^2 + 2}\right]^{\gamma/(\gamma-1)} \left(\frac{\gamma + 1}{2\gamma M^2 - \gamma + 1}\right)^{1/(\gamma-1)} \tag{1}$$

where M is the Mach number and γ the adiabatic coefficient (C_p/C_v).

If the Mach number is found to be uniform over the range in which we are interested, it is possible to calculate the temperature, pressure, and density in the flow via eqs 2−4, respectively.

$$\frac{T_0}{T} = 1 + \frac{\gamma - 1}{2}M^2 \tag{2}$$

$$\frac{p_0}{p} = \left(\frac{T_0}{T}\right)^{\gamma/(\gamma-1)} \tag{3}$$

$$\frac{\rho_0}{\rho} = \left(\frac{T_0}{T}\right)^{1/(\gamma-1)} \tag{4}$$

In eqs 2−4, T_0, p_0, and ρ_0 are the temperature, pressure, and density in the stagnation region, respectively, and T, p, and ρ are the temperature, pressure, and density in the gas beam, respectively.

In Figure 2a, the temperature that was calculated from the dynamic pressure measurements is plotted as a function of the axial distance l from the nozzle exit for a Laval nozzle that was designed to yield a temperature of 85 K (Mach 3.5). The agreement between the design and measured temperature and the gas density is good. The measured density as a function of the axial distance l from the nozzle exit is plotted in Figure 2b, and again, the density in the flow is close to the design density of $1 \times 10^{17}\ cm^{-3}$.

A three-dimensional impact pressure plot of the gas beam was recorded when the pressure impact detector was moved parallel and perpendicular to the flow. Such measurements have been found to be important for the full characterization of the flow conditions (Figure 3). The uniform gas flow downstream of the nozzle exit with a relatively constant temperature, density, and velocity was stable across 10−15 cm and for at least 200−300 μs.

In addition to the measurements above, the rotational temperatures of the OH radicals were recorded via LIF spectra. In general, the results from the dynamic pressure measurements and LIF spectra were in good agreement. Either the $Q_1(K)$ or the $S_{21}(K)$ lines of the LIF spectrum (Figure 4) were used for the temperature measurements. The time delay between the pump and the probe laser was set to 10 μs in this case.

III. Results and Discussion

A. Rate Constants for the Reactions of OH Radicals with Propene and Isoprene. The rate constants for the reactions of OH radicals with propene and isoprene have been measured at

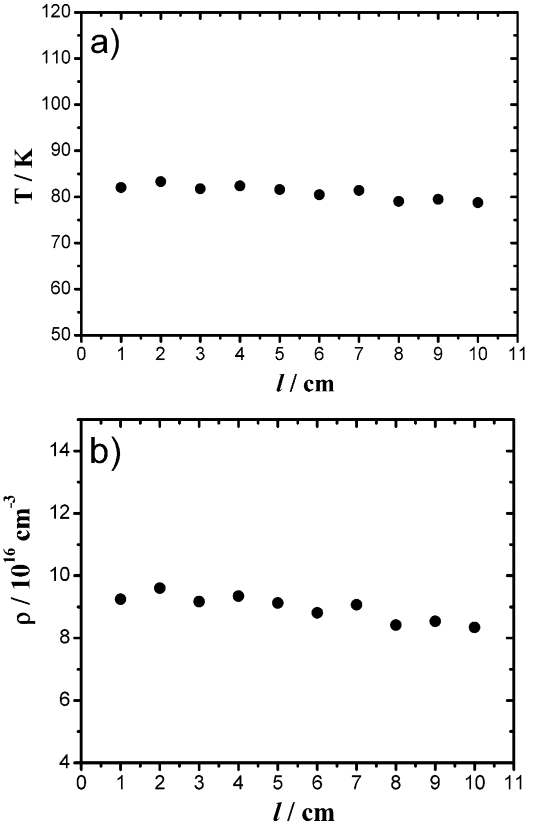

Figure 2. (a) Axial temperature profile from the dynamic pressure measurements. The distance from the nozzle exit is *l*. (b) Axial gas density profile from the dynamic pressure measurements. The distance between the nozzle exit and the detector, again, is *l*.

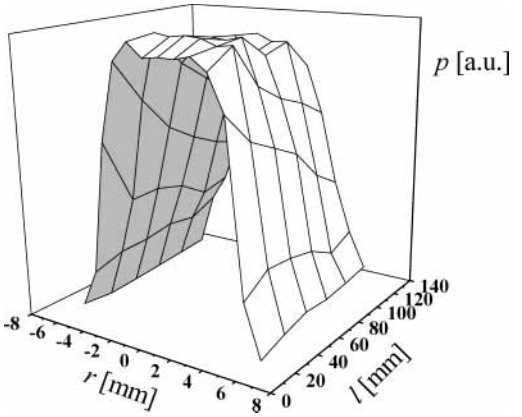

Figure 3. Three-dimensional impact pressure plot. The axial distance is *l*, and *r* is measured across the Laval nozzle expansion flow. For details, see the text.

temperatures between 58 and 300 K. Typical OH radical and reactant concentrations were approximately 1×10^{11} and 1×10^{14} cm^{-3}, respectively ($\rho_{tot} \approx 10^{17}$ cm^{-3}). We are, of course, aware of the problems arising from secondary chemistry reactions in this type of experiment;[42] however, in the present experimental conditions, we rule out the perturbations from the secondary reactions.

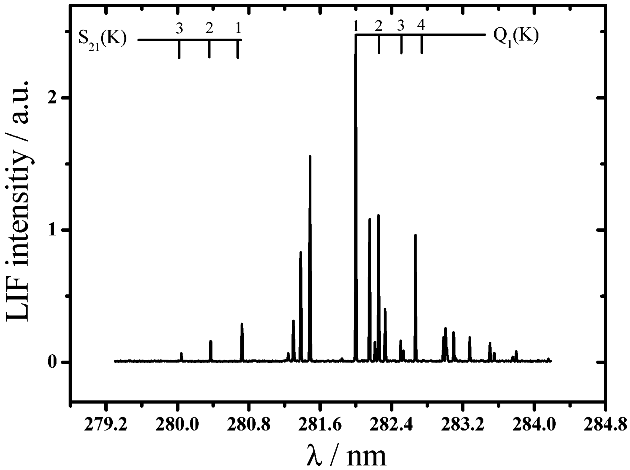

Figure 4. LIF spectra and assignments of OH radicals generated in the UV photodissociation of H_2O_2 at 193 nm.

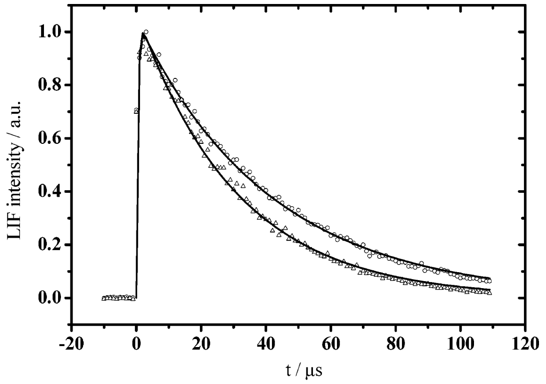

Figure 5. Typical exponential decays of the laser-induced fluorescence of the OH radicals in the reaction between propene and the OH radicals at different propene concentrations ($T = 71$ K, $\rho_{tot} = 9 \times 10^{16}$ cm^{-3}, $\rho_1 = 6.4 \times 10^{13}$ cm^{-3}, and $\rho_2 = 1.2 \times 10^{14}$ cm^{-3}).

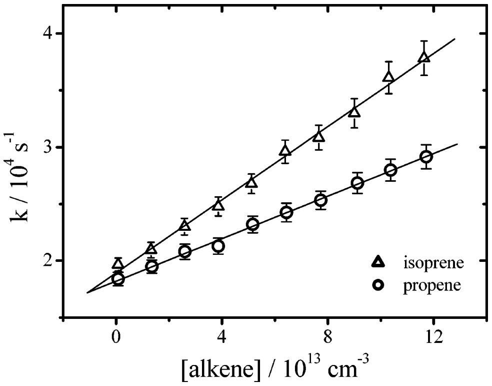

Figure 6. Plot of the pseudo-first-order rate constants vs the alkene concentration. The buffer gas in this case is nitrogen. The slope of the graph yields the second-order rate constant ($T = 71$ K, $\rho_{tot} = 9 \times 10^{16}$ cm^{-3}).

Figure 5 displays typical normalized experimental traces for the reaction between propene and OH radicals at different propene concentrations with H_2O_2 as the source of OH radicals ($T = 71$ K, $\rho_{tot} = 9 \times 10^{16}$ cm^{-3}, and $\rho_1/\rho_2 = 1.8$). The decay could be well-fitted with a single-exponential decay function. Significant deviations from the single-exponential behavior were not observed even in the early stages of the decay, where rotational relaxation may interfere. A plot of the pseudo-first-order rate constants versus the alkene concentration for both reactions ($T = 71$ K and $\rho_{tot} = 9 \times 10^{16}$ cm^{-3}) is given in Figure 6. From the slope of this graph, the second-order rate constant can be determined. The non-zero intercept of this graph may be attributed to the loss of OH due to the diffusion from the zone that was irradiated by the photolysis laser beam and/or a small OH loss from the reaction with H_2O_2. Figure 7 shows the rate constants of the reaction of OH with propene that were measured in this work (Table 2) together with the high-

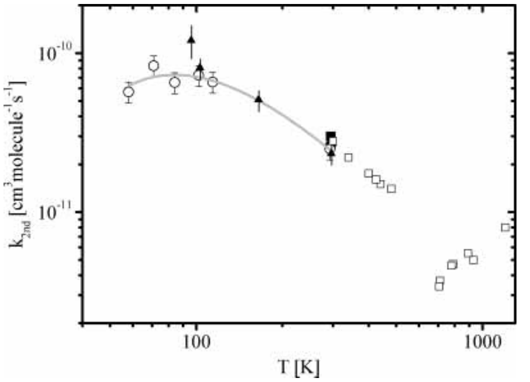

Figure 7. Comparison of the rate constants measured in this work and the previously measured rate constants for the reaction of propene with OH radicals. (■) Klein et al.,[43] (●) Atkinson and Aschmann,[44] (▲) Leone et al.,[3,23] (□) Tully and Goldsmith,[26] (○) this work, and (—) the empirical fit (to the expression $k(T) = A \times T^n \exp(\theta/T)$). For details, see the text.

TABLE 2: Measured Rate Constants for the Reaction of Propene with OH for Different Temperatures

temperature (K)	k ($\times 10^{-12}$ cm^3 s^{-1})
58	57 ± 9
71	83 ± 12
84	65 ± 10
102	73 ± 11
114	66 ± 10
293	25 ± 4

TABLE 3: Measured Rate Constants for the Reaction of Isoprene with OH for Different Temperatures

temperature (K)	k ($\times 10^{-12}$ cm^3 s^{-1})
58	78 ± 12
71	114 ± 17
84	98 ± 15
104	188 ± 28
114	168 ± 25
293	100 ± 15

temperature literature data plotted as a function of the temperature. From the literature data available for the reaction of OH with propene[23,26] and isoprene,[30] we conclude that both of the association reactions are in, or close to, their high-pressure limit at the temperatures and pressures accessed in this study.

The measured rate constants for the OH−propene reaction agree well with the data points from the Leone group,[3,23] and they are consistent with those (at higher temperatures) of Klein et al.,[43] Tully and Goldsmith,[26] and Atkinson and Aschmann.[44] In our present study, we have been able to extend the range of temperatures down to 58 K. The good agreement with the literature data shows that our pulsed Laval nozzle setup provides reliable low-temperature reaction conditions. At the same time, the results show that the generation of OH radicals from the 193 nm photolysis, which is our source of OH radicals at present, does not give results under our experimental conditions that are significantly different than the photolysis at 248 nm, the somewhat more preferred source for OH radicals in the literature.[24,25]

The new measurements confirm the negative temperature dependence of the reaction that was observed very recently.[3,23,26] However, the variation of the rate constants as a function of temperature appears to show a saturation behavior (see Figure 7) in the temperature ranges below 100 K; for example, the values at the lowest temperatures are not quite as high as one may expect from the extrapolation of the higher-temperature data.[3,23,26,43,44] Such a behavior has already been observed for other alkenes,[45] although the trend here is less pronounced. If we accept that the current data lie near the high-pressure limit, we may consider the temperature dependence of the reaction over the full range of temperature-dependent data available for this reaction. As seen in Figure 7 (between 400 and 700 K), the rate constants appear to decline by a factor of 4 before they rise again at higher temperatures due to the H atom abstraction. Therefore, the dramatic minimum in the rate constant near 700 K is another anomaly of the temperature dependence beyond the saturation effect at very low temperatures, which possibly means that no simple temperature dependence should be expected at all for this reaction.

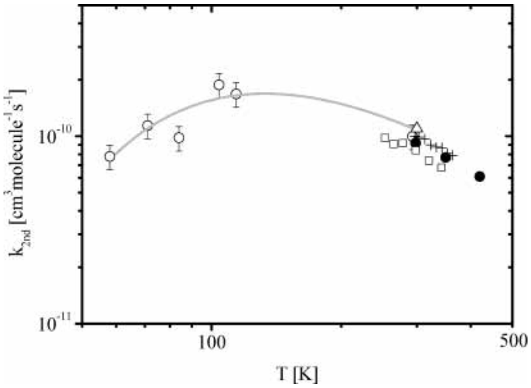

Figure 8. Comparison of the rate constants measured in this work with the previously measured rate constants for the reaction of isoprene with OH radicals. (+) Gill and Hites,[34] (●) Kleindienst et al.,[35] (□) Campuzano-Jost et al.,[36] (△) Stevens et al.,[46] (○) this work, and (—) the empirical fit (to the expression $k(T) = A \times T^n \exp(\theta/T)$). For details, see the text.

Figure 6 also shows the concentration dependence of the OH−isoprene reaction in comparison with the OH−propene reaction. The second-order rate constants for various temperatures are given in Figure 8 and are listed in Table 3. Also plotted in Figure 8 are data from the literature for the high-temperature region above 250 K.[34−36,46] Although our room-temperature data point is somewhat higher than that of the Kleindienst data, putting it more in accord with the Stevens value rather than the somewhat lower data from Hynes and co-workers, we find an overall reasonable agreement with the data (at higher temperatures) reported in the literature. With respect to the previous case, we confirmed that the negative temperature dependence[34−36] determined between 250 and 400 K continues to lower temperatures. What is surprising and somewhat unexpected is that the negative temperature dependence of the rate constant for higher temperatures saturates around 100 K and decreases again for lower temperatures, causing a pronounced maximum of the recombination rate constants.

Nevertheless, a maximum of the rate constant at low temperatures could have a trivial explanation, which we briefly want to address here. Due to the slightly different nozzle parameters (densities), the temperature dependence of the recombination rate could display density variations at different temperatures if the reaction was not in its high-pressure limit. Since the low-temperature recombination rates are close to the vibrational relaxation rate constant of OH ($v = 1$)[47] and since no correlation of the measured rates in Figures 7 and 8 with the flow densities given in Table 1 can be found, we think that such an explanation cannot apply here. Moreover, we have investigated other systems with the same set of nozzles and found that they exhibit a monotonic increase of the recombination rate as the temperature is lowered.

Another simple explanation for the observed trend in the temperature dependence would be a condensation/clustering of isoprene/propene at low temperatures. In such a case, k would not change but the reaction may simply be slowed due to a lower effective isoprene concentration. However, the linearity of plots such as those given in Figure 6 strongly argues against such an explanation.

For the purpose of kinetic modeling, it is useful to provide formulas that express how the rate coefficients, $k(T)$, for particular reactions vary with the temperature. Since the temperature dependence is often expressed in the form $k(T) = A \times T^n \exp(\theta/T)$, we have fitted our data (see Figures 7 and 8) to this form yielding the values of $A = 4.38 \times 10^{-6}$ cm^3 molecule^{-1} s^{-1}, $n = -2.03$, and $\theta = -170$ K for the OH−propene reaction and $A = 4.81 \times 10^{-6}$ cm^3 molecule^{-1} s^{-1}, $n = -1.74$, and $\theta = -232$ K for the OH−isoprene reaction. It should be stressed that this fitting is entirely empirical, and as a consequence, the use of the above formula outside the range of the measurements between 300 and 60 K should be avoided.

B. Temperature Dependence of the Reactions of OH Radicals with Unsaturated Hydrocarbons. The negative temperature dependence of the reactions investigated here is not unique. In fact, a remarkable number of reactions between radicals and unsaturated molecules, such as OH with butenes[45] and the classical CN and O_2 reaction,[14,48] have been found at low temperatures to be significantly faster than at room temperature.[1,2] A negative temperature dependence in combination with a maximum of the recombination constant of radicals at low temperatures has also been observed before, for example, in reactions of CH with various (unsaturated) hydrocarbons.[4] The effect has been investigated theoretically by Clary et al.,[49,50] and simple expressions for $T_{\max}$ values as a function of multipole moments and molecular parameters of the reactants have been suggested which, if applied to the present systems, predict significantly lower $T_{\max}$ values than were determined in this study.

The interpretation of the negative temperature dependence of the present systems and for these types of reactions in general is not clear, and there is some controversy about the correct qualitative picture. There are basically two approaches for the interpretation of this class of reactions which differ by the microscopic details of the potential energy surface in the entrance channel of the reaction, namely, the reaction coordinate.

A possible explanation for the observed negative temperature dependence for both reactions is that there is neither an adiabatic barrier nor a shallow well on the electronic potential that is associated with the adduct radical formation, and that the capture rates are governed mostly by the adiabatic capture on the long-range electrostatic potential of the lowest PES. As the temperature decreases, the transition-state region (rotational barriers), in the language of the loose transition-state theory, moves to larger interreactant separations and increases the reaction cross sections. Lowering the reactant rotational energy may also alter the probability of a reaction (in the case of strong anisotropy of the reaction) for a species remaining for a longer period of time in a favorable orientation, which would increase the overall thermal rate constant as the temperature is decreased. A saturation of the rate constants at low temperatures may be a consequence of the number of (electronic) surfaces which correlate with the separated reagents. If the reaction proceeds only on the lowest-potential energy surface, part of the negative temperature dependence which is observed between 400 and 100 K for both reactions may be attributed to the temperature-dependent thermal population of the electronic (spin−orbit) states of the OH radical. Below 100 K, however, essentially all of the OH will occupy the lower $^2\Pi_{3/2}$ spin−orbit component. The simplest explanation for a turnover of the temperature dependence of the recombination rate constant at even lower temperatures may be that any increase in the reaction cross section at low collision energies may be overcompensated by the decrease in relative velocity, and hence, the recombination rate may decrease as the temperature falls.[4] Such a scenario would, in principle, call for a rigorous treatment of the problem (including a calculation of all isomers) with the loose transition-state theory[5,6] in which either a Morse potential or the calculated PES points at short distances and a multipole expansion of the potential at large distances are employed to describe the reaction coordinate and in which energies and frequencies are taken from quantum chemistry. Recently, North and Zhang reported loose transition-state theory (RRKM) and Master equation calculations for the reaction of OH with isoprene based upon high-level quantum chemistry calculations, which match our experimental data at higher temperatures reasonably well.[30,51,52] However, our model calculations for individual isomers employing Troe's simplified statistical adiabatic channel model (assuming a simple Morse potential for the reaction coordinate, multipole interaction at larger distances, and energetics from quantum chemistry) could not satisfactorily reproduce the measured temperature dependence of the two reactions, namely, OH and propene and isoprene, over the extended range of temperatures considered here. While it was possible to qualitatively reproduce a negative temperature dependence at higher temperatures, the quantitative course of the rate constants as a function of the temperature could not be understood with this approach. The failure of this strategy may indicate that either more sophisticated variants of the SACM approach have to be employed (see ref 5 and refs cited therein) or the potential energy surface in this type of reaction differs from the assumed smooth barrierless potential.

It is known that anomalies and modifications of the potential may result from the interaction of the OH radicals with the double bonds of the unsaturated hydrocarbons that may form π-complexes (sometimes called "prereactive complexes"[53]) prior to the formation of what we will term σ-adducts (see Figure 9). This interaction leads to a shallow energy minimum that is separated from the larger potential well of the adducts by a more or less pronounced barrier. This adiabatic barrier may result naturally from (i) an avoided crossing of two potential energy surfaces,[54] (ii) the rotation of OH that is initially oriented in a way that the hydrogen atom points toward the double bond,[5] and/or (iii) the rehybridization of carbon atoms in the course of the reaction. The height of the barrier may be higher or lower than the asymptotic limit of the energies of the separated fragments (see Figure 9). The conjecture that weakly bound π-complexes exist in the addition of radicals to unsaturated hydrocarbons was first reported by Singleton and Cvetanovic for the reaction of oxygen atoms with olefins.[55] The existence of a prereactive complex in a shallow well and a barrier separating the π-complex and the σ-adduct leads to the two-transition-state scenario (see ref 54 and refs cited therein) shown schematically in Figure 9. In addition to the well and the barrier, which are not drawn to scale, we schematically show the microcanonical rate constants, $k(E)$, for the unimolecular decay of the complex back to the reactants and forward to the final adduct. Because the reverse reaction (characterized through a loose transition-state theory) is barrierless, the rate constant $k_{\mathrm{back}}(E)$ increases very rapidly with energy, whereas the forward reaction via a tight transition state shows a less steep rise of the rate constant $k_{\mathrm{forward}}(E)$. The $k(E)$ curves may intersect

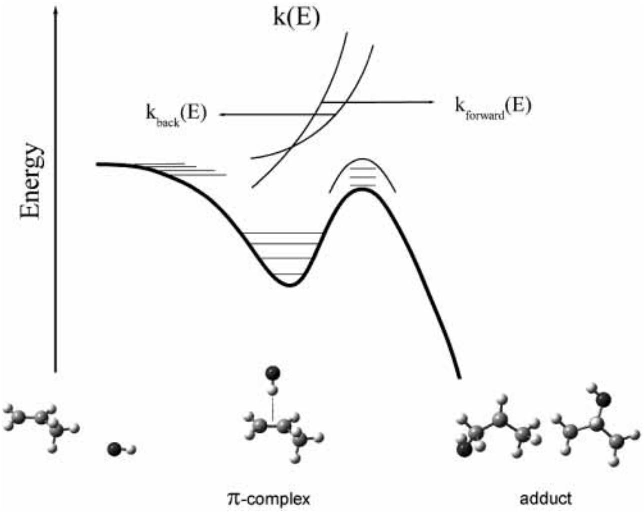

Figure 9. Schematic display of a potential energy scenario for the case of OH reacting with propene involving an adiabatic barrier and a shallow well, resulting from an avoided crossing of potential energy surfaces and interaction of the radical with the double bond of the alkene. The latter interaction may stabilize a weakly bound π-complex. Note: the barriers are not drawn to scale. The interplay of the relative barrier height compared to the asymptotic energy of the fragments and the relative rate constants for the forward and backward reaction of the π-complex may explain the negative temperature dependence of the reaction and the saturation at low temperatures (see the text).

depending upon the relative height of the barrier. Regardless, it is the branching ratio of the forward and backward reaction (defined by $k(E)$ divided by the sum over all $k(E)$) of the complex that determines the temperature dependence of the overall association reaction if this simple statistical scenario holds true. In Figure 9, we have depicted a scenario in which the barrier is lower than the asymptotic limit. For such a case, a negative temperature dependence of the recombination rate constant results naturally from the fact that at higher temperatures the complex preferably dissociates back to the educts, whereas at low temperatures the forward reaction dominates due to the lower barrier. A very intriguing feature of the present model is that it is the barrier height relative to the asymptotic limit that appears to determine whether the recombination rate increases, saturates, or turns over at very low temperatures.

It should be noted that there is some controversy about the presence or absence of a π-complex and, in particular, the barrier between the complex and the σ-adduct for the reactions of OH with propene and isoprene. The theoretical work of North and Zhang on the OH−isoprene reaction relies on a pure Morse potential connecting the adduct with the entrance channel and in addition reports finding no hint of a potential maximum in PES scans.[30,51,52] Other authors, including Abbat et al. (for OH and ethene[56]) and Donahue,[54] have argued for the existence of the π-complex based upon both computational and theoretical arguments. Recently, Diaz-Acosta et al.[57] found evidence of a π-complex in the OH−propene association reaction bound by a barrier of ~4 kcal relative to the asymptotic limit (E_∞) and with a barrier to the σ-complex that is ~2 kcal below E_∞. There is, however, evidence that the shape of the potential in the entrance channel of these reactions, in particular the depth of the well and the barrier, is sensitive to the level of the theory.[30]

IV. Summary and Conclusion

In summary, reactions of OH radicals with propene and isoprene in N_2 have been studied in the temperature range of 58−300 K in a pulsed Laval nozzle expansion. For these studies, a recently developed Laval nozzle expansion machine combined with laser-flash photolysis and laser-induced fluorescence detection has been employed. The good agreement between the measured data at room temperature and the literature data and the confirmation of a low temperature value for the OH−propene reaction near 100 K showed that the present setup produces reliable data. At the same time, it shows that the generation of OH radicals from 193 nm photolysis, which is our source of OH radicals at present, does not give results under our experimental conditions that are significantly different than those of the photolysis at 248 nm, the somewhat more preferred source for OH generation. The determined rate constants for OH radicals with excess propene and isoprene in the range of 2×10^{-11} to 2×10^{-10} cm^3 molecule^{-1} s^{-1} show a pronounced negative temperature dependence well above 100 K. Around 100 K, the recombination rate for propene saturates and may even decrease slightly. For isoprene, this effect is more pronounced such that a maximum of $k(T)$ around 100 K is visible.

The observed temperature dependence of the rate constants for both reactions is discussed within the framework of the loose transition-state theory and qualitatively explained with a simple two-transition-state model that assumes the existence of a π-complex in the entrance channel of the reaction and a small barrier that separates the complex and the σ-adduct. The temptation and fascination of the latter model is due to the fact that it may be able to naturally explain the observed temperature dependence of both title reactions in a qualitative fashion.

In conclusion, it is probably fair to state that the present measurements are certainly benchmark data for future theoretical studies on these systems. Both reactions are good examples that demonstrate the errors that are possible if high-temperature data are extrapolated toward very low temperatures. Due to the fact that the deviations from the extrapolated negative temperature dependence are at temperatures below 100 K (i.e., below atmospheric temperatures), the present findings will probably not affect atmospheric chemistry models; however, they will affect the theoretical microscopic understanding of these and other similar reactions which may or may not show anomalies in a different temperature range.

The decisive role of different isomers in the recombination reaction and the potential impact on its overall temperature dependence was not seen in the present study. It appears to be plausible that all isomers contribute to the overall association reaction, and that the relative recombination rates correlate with the stability of the σ-complexes.[30] Since the barrier energies for the interconversion between isomers is relatively high, the reaction of each isomer is probably independent of the others.

Acknowledgment. Financial support of this work by the Deutsche Forschungsgemeinschaft (SFB 357 “Molekulare Mechanismen Unimolekularer Prozesse”) is gratefully acknowledged. We also thank Professor J. Troe, Professor I. W. M. Smith, and Dr. I. R. Sims for helpful discussions, as well as R. Karunanandan for help with the experiment. B.A. and T.S. thank the Fonds der Chemischen Industrie for financial support.

References and Notes

(1) Smith, I. W. M. *Chem. Rev.* **2003**, *103*, 4549−4564.
(2) Sims, I. R.; Smith, I. W. M. *Annu. Rev. Phys. Chem.* **1995**, *46*, 109−137.
(3) Vakhtin, A. B.; Lee, S.; Heard, D. E.; Smith, I. W. M.; Leone, S. R. *J. Phys. Chem. A* **2001**, *105*, 7889−7895.
(4) Canosa, A.; Sims, I. R.; Travers, D.; Smith, I. W. M.; Rowe, B. R. *Astron. Astrophys.* **1997**, *323*, 644−651.
(5) Troe, J. *Chem. Rev.* **2003**, *103*, 4565−4576.

(6) Troe, J. In *Advances in Chemical Physics: Chemical Reactions and Their Control on the Femtosecond Time Scale*, XXth Solvay Conference on Chemistry; Gaspard, P., Burghard, I., Prigogine, I., Rice, S. A., Eds.; John Wiley & Sons: New York, 1997; Vol. 101.

(7) Dupeyrat, G.; Marquette, J. B.; Rowe, B. R. *Phys. Fluids* **1985**, *28*, 1273−1279.

(8) Atkinson, D. B.; Smith, M. A. *Rev. Sci. Instrum.* **1995**, *66*, 4434.

(9) Lee, S.; Hoobler, R. J.; Leone, S. R. *Rev. Sci. Instrum.* **2000**, *71*, 1816.

(10) Rowe, B. R.; Dupeyrat, G.; Marquette, J. B.; Gaucherel, P. *J. Chem. Phys.* **1984**, *80*, 4915−4921.

(11) Rowe, B. R.; Dupeyrat, G.; Marquette, J. B.; Smith, D.; Adams, N. G.; Ferguson, E. E. *J. Chem. Phys.* **1984**, *80*, 241.

(12) Rowe, B. R.; Marquette, J. B. *Int. J. Mass Spectrom. Ion Processes* **1987**, *80*, 239−254.

(13) Rowe, B. R.; Marquette, J. B.; Rebrion, C. *J. Chem. Soc., Faraday Trans.* **1989**, *80*, 1631.

(14) Sims, I. R.; Queffelec, J.-L.; Defrance, A.; Rebrion-Rowe, C.; Travers, D.; Bocherel, P.; Rowe, B. R.; Smith, I. W. M. *J. Chem. Phys.* **1994**, *100*, 4229−4241.

(15) Brownsword, R. A.; Canosa, A.; Rowe, B. R.; Sims, I. R.; Smith, I. W. M.; Stewart, D. W. A.; Symonds, A. C.; Travers, D. *J. Chem. Phys.* **1997**, *106*, 7662−7677.

(16) Chastaing, D.; James, P. L.; Smith, I. W. M. *Faraday Discuss.* **1998**, *109*, 165.

(17) Chastaing, D.; James, P. L.; Sims, I. R.; Smith, I. W. M. *Phys. Chem. Chem. Phys.* **1999**, *1*, 2247.

(18) Atkinson, D. B.; Smith, M. A. *J. Phys. Chem.* **1994**, *98*, 5797.

(19) Atkinson, D. B.; Jaramillo, V. I.; Smith, M. A. *J. Phys. Chem. A* **1997**, *101*, 3356−3359.

(20) Vakhtin, A. B.; Heard, D. E.; Smith, I. W. M.; Leone, S. R. *Chem. Phys. Lett.* **2001**, *344*, 317−324.

(21) Vakhtin, A. B.; Heard, D. E.; Smith, I. W. M.; Leone, S. R. *Chem. Phys. Lett.* **2001**, *348*, 21−26.

(22) Lee, S.; Leone, S. R. *Chem. Phys. Lett.* **2000**, *329*, 443.

(23) Vakhtin, A. B.; Murphy, J. E.; Leone, S. R. *J. Phys. Chem. A* **2003**, *107*, 10055−10062.

(24) Atkinson, R. *Chem. Rev.* **1985**, *85*, 69−201.

(25) Atkinson, R.; Baulch, G. L.; Hampson, R. F. J.; Kerr, J. A.; Rossi, M. J.; Troe, J. *J. Phys. Chem. Ref. Data* **1997**, *26*, 521.

(26) Tully, F. P.; Goldsmith, J. E. M. *Chem. Phys. Lett.* **1985**, *116*, 345.

(27) Rasmussen, R. S.; Khallil, M. A. *J. Geophys. Res.* **1988**, *93*, 1417.

(28) Tuazon, E. C.; Atkinson, R. *Int. J. Chem. Kinet.* **1990**, *22*, 1221.

(29) Paulson, S. E.; Flagan, R. C.; Seinfeld, J. H. *Int. J. Chem. Kinet.* **1992**, *24*, 79.

(30) McGivern, W. S.; Suh, I.; Clinkenbeard, A. D.; Zhang, R.; North, S. W. *J. Phys. Chem. A* **2000**, *104*, 6609.

(31) Chuong, B.; Stevens, P. S. *J. Phys. Chem. A* **2000**, *104*, 5230−5237.

(32) Stevens, P. S.; Seymour, E.; Li, Z. *J. Phys. Chem. A* **2000**, *104*, 5989−5997.

(33) Zhang, R.; Suh, I.; Lei, W.; Clinkenbeard, A. D.; North, S. W. *J. Geophys. Res.* **2000**, *D20*, 24627.

(34) Gill, K. J.; Hites, R. A. *J. Phys. Chem. A* **2002**, *106*, 2538.

(35) Kleindienst, T. E.; Harris, G. W.; Pitts, J. N. *Environ. Sci. Technol.* **1982**, *16*, 844−846.

(36) Campuzano-Jost, P.; Williams, M. B.; D'Ottone, L.; Hynes, A. *Geophys. Res. Lett.* **2000**, *27*, 693−696.

(37) Moger, W. C.; Ramsay, D. B. Report No. AEDC-TDR-64-110, Arnold Engineering Development Center: Tullahoma, TN, 1964.

(38) Atkinson, R.; Baulch, D. L.; Cox, R. A.; Hampson, R. F., Jr.; Kerr, J. A.; Troe, J. *J. Phys. Chem. Ref. Data* **1992**, *21*, 1174.

(39) Vaghjiani, G. L.; Ravishankara, A. R. *J. Chem. Phys.* **1990**, *92*, 996−1003.

(40) Vaghjiani, G. L.; Turnipseed, A. A.; Warren, R. F.; Ravishankara, A. R. *J. Chem. Phys.* **1992**, *96*, 5878−5886.

(41) Spangenberg, T.; Hansmann, B.; Koehler, S.; Abel, B. Unpublished results.

(42) Donahue, N. M. *J. Phys. Chem.* **1996**, *100*, 17855.

(43) Klein, T.; Barnes, I.; Fink, E. H.; Zabel, F. *J. Phys. Chem.* **1984**, *88*, 5020−5025.

(44) Atkinson, R.; Aschmann, S. M. *Int. J. Chem. Kinet.* **1984**, *16*, 1175−1186.

(45) Sims, I. R.; Smith, I. W. M.; Bocherel, P.; Defrance, A.; Travers, D.; Rowe, B. R. *J. Chem. Soc., Faraday Trans.* **1994**, *90*, 1473.

(46) Stevens, P.; L'Esperance, D.; Chuong, B.; Martin, G. *Int. J. Chem. Kinet.* **1999**, *31*, 637.

(47) Sims, I. R.; Queffelec, J.-L.; Travers, D.; Rowe, B. R.; Herbert, L. B.; Karthäuser, J.; Smith, I. W. M. *Chem. Phys. Lett.* **1993**, *211*, 461−468.

(48) Sims, I. R.; Smith, I. W. M. *Chem. Phys. Lett.* **1988**, *151*, 481.

(49) Clary, D. C. *Annu. Rev. Phys. Chem.* **1990**, *41*, 61.

(50) Clary, D. C.; Stoecklin, T. S.; Wickham, A. G. *J. Chem. Soc., Faraday Trans.* **1993**, *79*, 2185.

(51) Park, J.; Stephens, J. C.; Zhang, R.; North, S. W. *J. Phys. Chem. A* **2003**, *107*, 6408.

(52) Lei, W.; Zhang, R. *J. Chem. Phys.* **2000**, *113*, 5354.

(53) Hansen, J. C.; Fransisco, J. S. *ChemPhysChem* **2002**, *3*, 833−840.

(54) Donahue, N. M. *Chem. Rev.* **2003**, *103*, 4593.

(55) Singleton, D. L.; Cvetanovic, R. J. *J. Am. Chem. Soc.* **1976**, *98*, 6812−6819.

(56) Abbat, J. P. D.; Anderson, J. G. *J. Phys. Chem.* **1991**, *95*, 2382.

(57) Diaz-Acosta, I.; Alvarez-Idaboy, R.; Vivier-Bunge, A. *Int. J. Chem. Kinet.* **1999**, *31*, 29.